PHYSICAL REVIEW A **87**, 041803(R) (2013)

Diamond lattice photonic crystals from rolled-up membranes

Matthew R. Jorgensen,[1,*] Silvia Giudicatti,[1] and Oliver G. Schmidt[1,2]

[1]*Institute for Integrative Nanosciences, IFW Dresden, Helmholtzstrasse 20, 01069 Dresden, Germany*

[2]*Material Systems for Nanoelectronics, Chemnitz University of Technology, Reichenhainer Strasse 70, 09107 Chemnitz, Germany*

(Received 8 January 2013; published 18 April 2013)

A method is suggested for the fabrication of three-dimensional photonic crystals operating in the visible by rolling patterned prestressed membranes. A variety of architectures accessible using this fabrication scheme, including ⟨111⟩ and ⟨100⟩ diamond structures, were theoretically examined and optimized using photonic-band and density-of-optical-states calculations. The influence that finite size and bending have on a band gap was explored using a finite-element analysis of a two-dimensional triangular lattice of air holes.

DOI: 10.1103/PhysRevA.87.041803 PACS number(s): 42.70.Qs, 81.07.−b

Many emerging technologies rely on the ability to control light and emitters in novel and precise ways. Strategies allowing light slowing, trapping, and routing, as well as control of spontaneous emission are of fundamental importance for solar energy conversion, lasing, and quantum information processing [1–7]. These effects can be related to the photonic density of states (DOS) through dispersion relations and Fermi's golden rule [8,9]. Diverse methods to control DOS have been researched including photonic crystals (PCs)—materials with a dielectric periodicity on the order of interacting wavelengths of light—as well as optical cavities and plasmonics [10–14]. Of these methods, PCs are advantageous because of their broad bandwidth of DOS inhibition, and, since modifications are a bulk effect, they are not limited by small cavity volumes.

Unfortunately, fabrication of three-dimensional (3D) PCs with lattice parameters suitable for the visible spectral range has proven difficult. While there have been interesting examples of structures produced using colloidal self-assembly [15–17] which have expanded fundamental understanding in the field, these PCs are limited to just the few lattice types accessible by self-assembly and have been theoretically and experimentally demonstrated to only moderately modify the DOS [17–19]. Remarkable work has been done fabricating diamond-based PCs functioning at wavelengths in the near-IR and longer using direct writing, holography, and layer-by-layer methods [20–26]. Recently there have been impressive examples of TiO_2 and GaN woodpile PCs produced using layer-by-layer techniques that operate in the visible [27,28]. However, these methods are very difficult to achieve experimentally, having been realized up to only nine layers and with directional band gaps (PBGs). Other diamond-based PCs operating in the visible have been fabricated via a biotemplating route [29], and showed a strong effect on DOS [5]. While biotemplating remains an interesting alternative to more conventional fabrication methods, it is limited by the inherent defects and small size of natural PCs.

Rolled-up nanotechnology [30,31] has been developing discretely from PC research. Rapid progress in this still-young field has yielded fascinating cylindrical structures including microjets [32], optical microcavities [33], batteries [34,35], integrated optofluidic sensors [36], and others from a wide variety of materials including titania [37,38]. In this Rapid Communication, we propose and theoretically discuss PCs fabricated by rolling prepatterned, prestrained membranes, as shown in Fig. 1.

Methods of fabricating rolled-up architectures have been discussed in detail in the literature [38]. Briefly, a sacrificial layer is patterned using photolithography upon which the membrane material to be rolled may be deposited in a manner to introduce strain, and at an angle to leave a ballistic shadow that allows for the subsequent removal of the sacrificial layer [38]. When the sacrificial layer is removed, the strain in the membrane is relieved by rolling it in a controlled direction. If a strained two-dimensional (2D) membrane is patterned using *e*-beam lithography and plasma or reactive ion etching, a 3D PC would result upon rolling, as shown schematically in Fig. 1(a). Due to the many materials—and their combinations—allowed by the rolling process, the control permitted by the deposition process, and the variety of 2D lattices available, a broad family of 3D PCs including ⟨100⟩ and ⟨111⟩ diamond lattices are accessible, as shown in Figs. 1(b) and 1(c).

We classify the members of this family based on the controllable physical parameters. For a given in-plane lattice type, both symmetric ($\mathbf{a1} = \mathbf{a2}$) and nonsymmetric ($\mathbf{a1} \neq \mathbf{a2}$) cases should be considered, where **a1** and **a2** are the primitive vectors of the lattice. For a given 2D geometry, different rolling directions were investigated. The rolling process layers the 2D PC on itself, creating a 3D system composed of stacked patterned windings. The 3D structure is strictly related to the thickness and stacking conditions of the rolled film.

Even with a defined 3D lattice type, the properties of the crystal structure can be adjusted by several other parameters. For example, control over hole radius (filling fraction), hole shapes, etch profiles, and partial etching is available. One of the most critical parameters, the refractive index (n_{ref}) of the dielectric material, can be at least partially controlled during the deposition and subsequent postrolling processes. In this Rapid Communication we focus our attention on titania, which has a n_{ref} that varies from about 2.0 up to 2.9 depending on the crystal phase composition and material porosity. We use the approximate high end of its reported n_{ref} ($n_{\text{ref}} = 2.9$) [39] in many of our calculations which investigate the impact various structural parameters have on band features. Its high n_{ref}, transparency, and semiconducting behavior make titania

*Corresponding author: m.jorgensen@ifw-dresden.de

 ©2013 American Physical Society

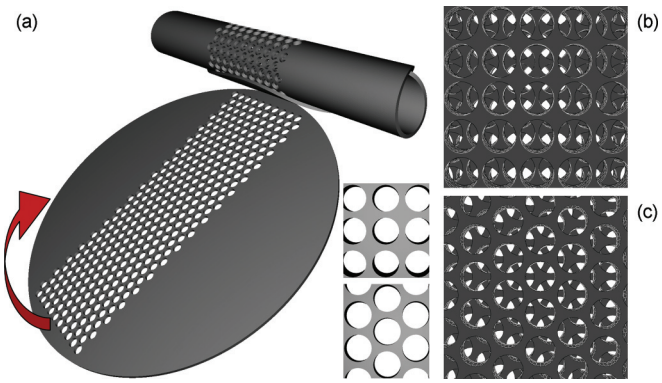

FIG. 1. (Color online) (a) A 3D PC could be rolled up from a strained membrane prepatterned with a square or triangular lattice (insets). The size of the 2D lattice constant, hole diameter, and rolled-up tube diameter are scaled by a factor of 25 relative to the large circular pattern for visibility. (b) ⟨100⟩ diamond structure accessible by rolling a square. (c) ⟨111⟩ diamondlike structure accessible by rolling a triangular lattice in the $\mathbf{a1}+\mathbf{a2}$ lattice directions.

a promising candidate for photonics applications at visible frequencies. Alternatively, the PC n_{ref} may be modified by changing the composition of the membrane. For example, instead of a simple titania film, a membrane composed of a silica/titania bilayer can be rolled. By controlling the silica percentage, the average n_{ref} can be tuned.

Thanks to fabrication flexibility, many interesting PC structures are possible. To identify the most promising PCs for the achievement of strong modification of DOS, a theoretical investigation of several lattice types was performed using MIT's Photonic Bands (MPB) [40]. After a preliminary analysis, the structural parameters were optimized for the most promising crystals. The DOS was calculated using a house-written program based on Ref. [8].

Of the PC structures we tested based on a square 2D lattice, a ⟨100⟩ diamond structure produced the broadest full PBG. The ⟨100⟩ diamond structure [41,42] can be obtained by rolling a 2D square lattice which is offset one half a period alternating along the **a1** and **a2** directions with every winding of the rolled-up tube. A top view of the resulting 3D structure is shown in Fig. 1(b). To be a "true diamond" structure, the film thickness and cylinder spacing are constrained to $0.25a$ and $a/\sqrt{2}$, respectively. However, the hole radius, shape, and etching profile remain free. For our system, the hole radius resulting in the widest full PBG (8.3%) is $0.49a/\sqrt{2}$. However, such a large radius would lead to extremely thin titania veins among adjacent holes, resulting in a mechanically unstable 2D membrane, probably preventing the rolling process. The performed simulations show that reducing the cylinder's radius to $0.45a/\sqrt{2}$ only reduces the gap to 7.1%, while making the fabrication process more feasible. After optimizing the hole radius, n_{ref} of titania was varied to find the minimum required. For this structure, a full PBG opens at $n_{\text{ref}} = 2.3$, which is easily accessible with titania using e-beam deposition techniques [43]. Therefore, the calculated band structure features a full PBG with a width up to 7.1% ($n_{\text{ref}} = 2.9$) centered at $0.54\,c/a$. The results including DOS corresponding to the high-end n_{ref} are reported in Fig. 2(a).

The ⟨111⟩ diamondlike structure [41] is accessible by rolling a symmetrical triangular lattice along the $(\mathbf{a1}+\mathbf{a2})$ direction, so that an *ABC* stacked PC results, as shown in Fig. 1(c). Under these more relaxed conditions, several parameters are adjustable to achieve a fine-tuned structure. Figures 2(b)–2(d) report some of the key results of our parameter optimization related to this lattice type. The difference between the minimum of the third band and the maximum of the second one was chosen as an indicator of optimization. Throughout the adjustment procedures, each partial PBG and the overall PBG (or the lack thereof) were monitored to probe the influence different structural features have on the directional gaps. Figure 2(b) shows a change in the membrane thickness, while *ABC* stacking is maintained. It was found that an increase in the membrane thickness results in the opening of one important directional gap $(L' - M')$ while closing another $(U' - L'')$, where L and M (along with their symmetry equivalent primes) correspond to the directions normal to the PC surface and the $\mathbf{a1}+\mathbf{a2}$ directions, respectively. The U directions correspond to out-of-plane skew angles through the structure. A membrane thickness of $0.72a$ represents the best compromise between the two competing effects, as shown in Fig. 2(b), where the overall PBG is effectively determined by these two directional bands. Therefore, for this thickness value, the radius of the cylindrical holes was optimized, as shown in Fig. 2(c). The partial PBGs come closest to overlapping when the radius is equal to $0.42a$, resulting in the band diagram shown as the inset in Fig. 2(d). Even though there is not quite a full PBG, many directional gaps overlap to make a 3.2% wide pseudogap centered at $0.4\,c/a$. The presence of the overlapping stop gaps in the band structure are also reflected in the calculated DOS distribution shown in Fig. 2(d); within the pseudogap frequency range, the DOS is reduced by 68%.

Other ways to customize the band gap were explored, though none of them produce a full PBG in the ⟨111⟩ diamondlike structures. Conical-shaped as well as partially etched holes widen certain directional gaps while closing others. By replacing the simple titania membrane with a silica/titania bilayer it is possible to improve the directional gap over the two important $U' - L''$ and $M' - L'$ bands, though this is counteracted by other directions. It was found that a full PBG would be opened in the ⟨111⟩ structure with a membrane refractive index larger than 4.2. This value is significantly higher than the refractive index of titania, but in the range of many widely used semiconductor materials that could be useful for other applications outside of the visible.

While ⟨111⟩ diamondlike structures accessible by rolling do not produce a full PBG, there are some potential advantages. The ⟨111⟩ stacked structures require no offsetting of the 2D lattice, making it easier to fabricate. Compared to the ⟨100⟩ diamond lattice, the ⟨111⟩ structure has a much thicker membrane that should result in greater mechanical stability. Finally, the ⟨111⟩ diamondlike lattice has many customizable band features, which are useful in the case of rolled-up structures where transmission of light in only certain directions is desirable.

Fabrication of PCs via a rolling process immediately raises questions regarding the impact that bending has on PC properties. PC structures are typically characterized by their photonic bands and band gaps, terms that apply when

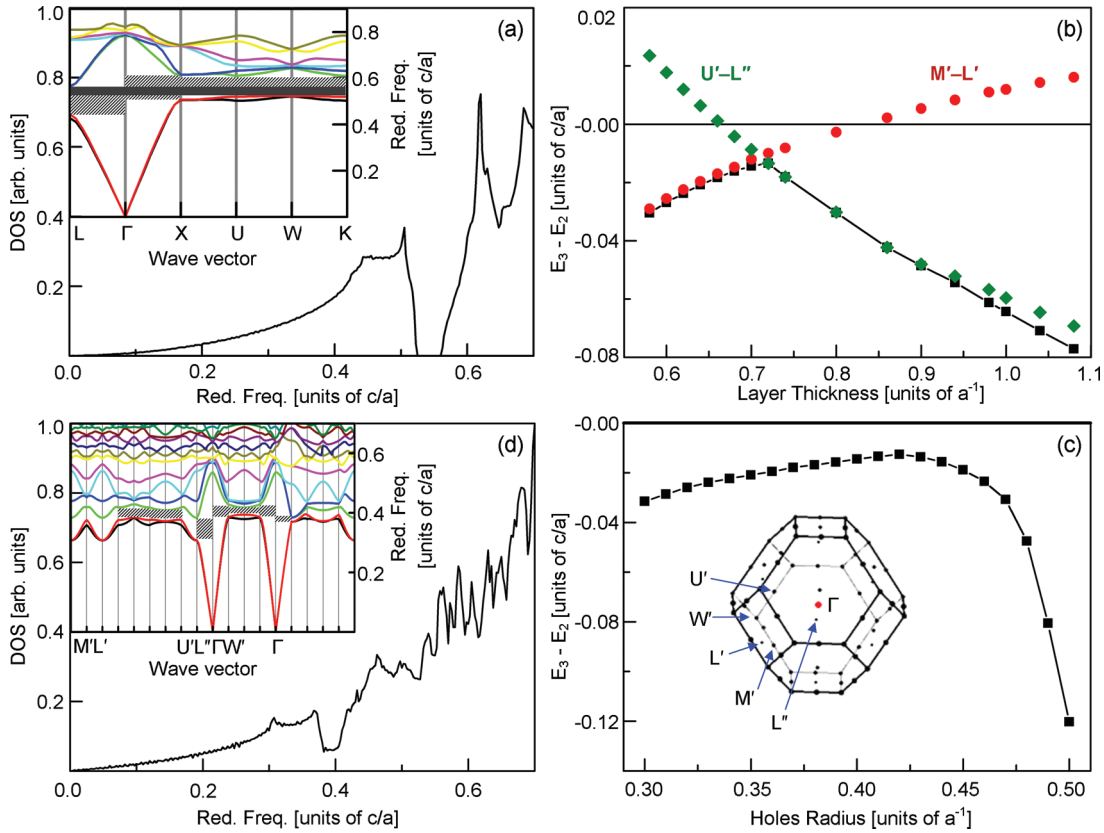

FIG. 2. (Color online) (a) Band diagram (inset) and density of optical states for the ⟨100⟩ diamond structure. The partial gaps are indicated by dashed lines and the overlapping stop gaps are marked by a dark gray region. (b), (c) Optimization procedure for the ⟨111⟩ diamond structure. (b) The difference between the minimum of the third band and the maximum of the second band spanning the entire band diagram (solid line) and separately for two different propagation directions as a function of membrane thickness. The bands spanning $M' - L'$ and $U' - L''$ prevent the appearance of a full PBG. (c) The difference between the minimum of the third band and the maximum of the second band calculated over the entire band diagram as a function of the cylindrical hole radius. (d) Band diagram (inset) and density of optical states (DOS) for the system characterized by a membrane thickness t= $0.72a$ and hole radius $r = 0.42a$. The overlapping directional stop gaps are marked by dashed regions.

conditions for Bloch's theorem are satisfied. If a PC is limited in size, or bent, then the concepts of bands and band gaps lose their meaning. To explore this issue, we investigated a 2D representation of our PC using both a Bloch-iterative plane wave expansion, and using finite-element analysis (FEA).

The photonic bands correlating to a triangular lattice of air holes ($r = 0.42a$) surrounded by a n_{ref} of 2.9 were calculated under the assumptions of linearity and infinite size using MPB. A segment of this band structure, the region corresponding to light with **k** vectors pointing in the Γ-M direction, is shown in Fig. 3. In this direction the triangular lattice of air holes has a very broad PBG centered at 0.36 c/a and two other small gaps 0.91 and 0.98 c/a.

A limited version of the same structure, 16 × 20 periods, was modeled for calculation using commercially available FEA software so that transmission of transverse electric (TE) polarized light through the structure was measured. This 2D slice of the structure, a triangular lattice of air holes, was chosen because it conserves the filling fraction of the full 3D structure. An excellent agreement was found between the simulated transmission FEA results and calculated band structures, as shown in Fig. 3(a). The same calculation was repeated, having the light pass through a variety of periods or layers. It was found that the transmission was reduced to less than 1% after only six periods, providing a useful guideline for the number of windings. If light is to be guided through the tube's hollow center, six windings is enough; 12 windings would be needed to effectively inhibit spontaneous emission. Figure 3(b) shows the calculated transmission for one to eight periods or layers, in comparison with a 16-layer calculation.

The impact bending has on a PBG was explored in a similar manner, and is summarized in Fig. 4. The transmission spectrum was simulated as the lattice was distorted and bent over a range of radii. To achieve the bend, the original structure was compressed towards the center of an arc with radius r/a, as shown in Fig. 4(a). It was found that the PBG was remarkably robust to bending, maintaining an almost complete blocking of light even at tight radii, down to $10a$ or 2.5 μm if the structure has a lattice constant appropriate for the visible spectrum. Rolled-up microtube radii are typically in the range of 10–25 μm, though they can be tuned over a much larger range. The PBG center shifts by only 1%. The height of the transmission peaks at the band edge decreases more significantly however, as shown in Fig. 4(b), suggesting

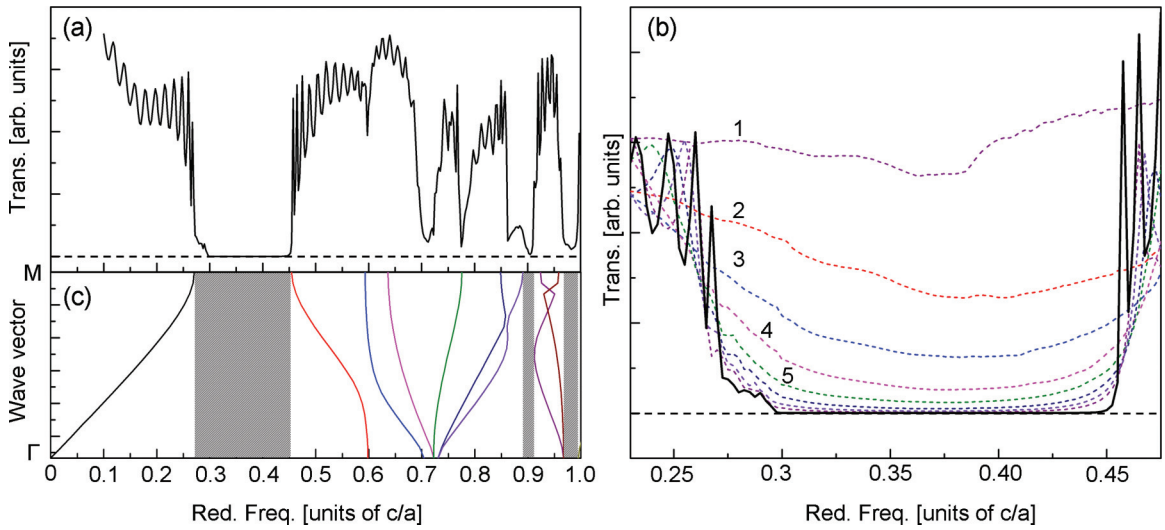

FIG. 3. (Color online) (a) Transmission spectrum, calculated using FEA, through 16 periods of a 2D triangular lattice of air holes. The transmission spectrum correlates nicely with the corresponding band diagram shown in (c), which was calculated assuming an infinite and linear lattice. (b) Calculated transmission spectrum around the large PBG through several different periods of a triangular lattice of air holes, as indicated on the graph. A lattice with only six periods reduces the transmitted light to less than 1%. The solid line is the same data shown in (a).

increased scattering. Therefore, it appears that bending of a PC can *destroy* optical modes, but not create them.

These promising results of FEA encourage the pursuit of rolled-up PCs. In our 2D simulations, only a few periods are needed to achieve nearly complete suppression of optical modes in transmission. Further, the PBG in a triangular lattice of air holes is maintained even with tight bending.

We have proposed a method for the fabrication of 3D PCs. Prestrained membranes could be patterned using *e*-beam lithography and etching techniques, and then subsequently allowed to roll. This method provides broad control over structural parameters, permitting the creation of a wide range of 3D PCs including the diamond and diamondlike structures. We have explored some of these possible structures according to their 2D lattice type, rolling direction, and stacking. Interestingly, we found that a full band gap was not possible using our technique for ⟨111⟩ stacked diamondlike lattices below n_{ref} of 4.2. However, a full PBG is found in a ⟨100⟩ stacked diamond lattice above n_{ref} of about 2.3, which is accessible in the visible. Promising results regarding the impact that finite size and bending have on a PBG were obtained using FEA.

Fabrication of 3D PCs by rolling 2D membranes is an interesting approach to some of the old problems facing the creation of full PBG PCs operating in the visible. Fabrication of rolled structures can be achieved in parallel, and the resulting hollow structures can be integrated into more complicated devices, making these potential structures ideal for on-chip laser light sources, solar energy collectors, and other optical elements. Rolled membranes are already used in a variety

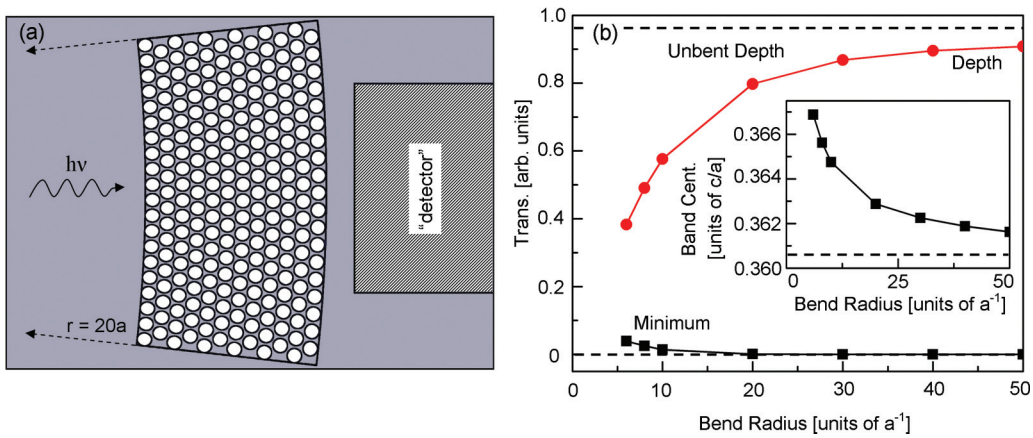

FIG. 4. (Color online) (a) Schematic of model used in FEA calculations. Light enters from the left and is incident on a triangular lattice of air holes bent over a radius. The intensity of light on the other side relative to the incoming light defines the transmission. (b) Variation of the difference or depth between maximum band-edge transmission and minimum PBG transmission as a 2D lattice of air holes is bent. The minimum transmission remains largely unchanged. However, the transmission through the band edges is reduced, suggesting the destruction of optical modes. The PBG center, shown in the inset, changes very slightly during bending.

of capacities as optical microcavities. By combining PCs with rolled optical microcavity waveguides, chiral structures could be made with optical effects that are interesting from a fundamental perspective.

[1] H.-G. Park *et al.*, Science **305**, 1444 (2004).
[2] M. H. Qi *et al.*, Nature (London) **429**, 538 (2004).
[3] T. Baba, Nat. Photonics **2**, 465 (2008).
[4] D. M. Callahan, J. N. Munday, and H. A. Atwater, Nano Lett. **12**, 214 (2011).
[5] M. R. Jorgensen, J. W. Galusha, and M. H. Bartl, Phys. Rev. Lett. **107**, 143902 (2011).
[6] Z.-H. Chen, S. Hellström, Z.-Y. Yu, and Y. Fu, Sol. Energy Mater. Sol. Cells **99**, 316 (2012).
[7] J. Hagemeier *et al.*, Opt. Express **20**, 24714 (2012).
[8] K. Busch and S. John, Phys. Rev. E **58**, 3896 (1998).
[9] R. Loudon, *The Quantum Theory of Light* (Oxford University Press, New York, 2000).
[10] S. John, Phys. Rev. Lett. **58**, 2486 (1987).
[11] E. Yablonovitch, Phys. Rev. Lett. **58**, 2059 (1987).
[12] K. J. Vahala, Nature (London) **424**, 839 (2003).
[13] K. Hennessy *et al.*, Nature (London) **445**, 896 (2007).
[14] G. Vecchi, V. Giannini, and J. Gómez Rivas, Phys. Rev. Lett. **102**, 146807 (2009).
[15] D. J. Norris *et al.*, Adv. Mater. **16**, 1393 (2004).
[16] J. W. Galusha, C. K. Tsung, G. D. Stucky, and M. H. Bartl, Chem. Mater. **20**, 4925 (2008).
[17] I. S. Nikolaev, W. L. Vos, and A. F. Koenderink, J. Opt. Soc. Am. B **26**, 987 (2009).
[18] I. S. Nikolaev, P. Lodahl, and W. L. Vos, J. Phys. Chem. C **112**, 7250 (2008).
[19] P. Lodahl *et al.*, Nature (London) **430**, 654 (2004).
[20] A. Blanco *et al.*, Nature (London) **405**, 437 (2000).
[21] F. García-Santamaría *et al.*, Adv. Mater. **19**, 1567 (2007).
[22] S. Lin *et al.*, Nature (London) **394**, 251 (1998).
[23] S. Noda, K. Tomoda, N. Yamamoto, and A. Chutinan, Science **289**, 604 (2000).
[24] M. Maldovan, E. L. Thomas, and C. W. Carter, Appl. Phys. Lett. **84**, 362 (2004).
[25] X. Z. B. Y. A. Vlasov, J. C. Sturm, and D. J. Norris, Nature (London) **414**, 289 (2001).
[26] S. Wong *et al.*, Adv. Mater. **18**, 265 (2006).
[27] G. Subramania, Y.-J. Lee, A. J. Fischer, and D. D. Koleske, Adv. Mater. **22**, 487 (2010).
[28] G. Subramania *et al.*, Nano Lett. **11**, 4591 (2011).
[29] J. W. Galusha, M. R. Jorgensen, and M. H. Bartl, Adv. Mater. **22**, 107 (2010).
[30] O. G. Schmidt and K. Eberl, Nature (London) **410**, 168 (2001).
[31] V. Y. Prinz *et al.*, Physica E **6**, 828 (2000).
[32] Y. F. Mei *et al.*, Adv. Mater. **20**, 4085 (2008).
[33] T. Kipp, H. Welsch, Ch. Strelow, Ch. Heyn, and D. Heitmann, Phys. Rev. Lett. **96**, 077403 (2006).
[34] C. C. Bof Bufon *et al.*, Nano Lett. **10**, 2506 (2010).
[35] H. X. Ji, Y. F. Mei, and O. G. Schmidt, Chem. Commun. **46**, 3881 (2010).
[36] E. J. Smith *et al.*, Lab Chip **12**, 1917 (2012).
[37] J. Wang *et al.*, Opt. Express **20**, 18555 (2012).
[38] Y. F. Mei, A. A. Solovev, S. Sanchez, and O. G. Schmidt, Chem. Soc. Rev. **40**, 2109 (2011).
[39] M. R. Shenoy and R. M. de la Rue, IEE Proc.-J: Optoelectron. **139**, 163 (1992).
[40] S. Johnson and J. Joannopoulos, Opt. Express **8**, 173 (2001).
[41] M. Maldovan and E. L. Thomas, Nat. Mater. **3**, 593 (2004).
[42] L. Lu *et al.*, Opt. Lett. **37**, 4726 (2012).
[43] P. Löbl, M. Huppertz, and D. Mergel, Thin Solid Films **251**, 72 (1994).